analytical chemistry

Article

pubs.acs.org/ac

Sensing Small Molecule Interactions with Lipid Membranes by Local pH Modulation

Da Huang,[†] Tao Zhao,[‡,∥] Wei Xu,[†] Tinglu Yang,[†,‡] and Paul S. Cremer*[,†,‡,§]

[‡]Department of Chemistry and [§]Department of Biochemistry and Molecular Biology, Penn State University, University Park, PA 16802

[†]Department of Chemistry, Texas A&M University, College Station, TX 77843

[∥]College of Chemistry and Chemical Engineering, Shanghai University of Engineering Science, Shanghai 201620, China

Supporting Information

ABSTRACT: Herein, we utilized a label-free sensing platform based on pH modulation to detect the interactions between tetracaine, a positively charged small molecule used as a local anesthetic, and planar supported lipid bilayers (SLBs). The SLBs were patterned inside a flow cell, allowing for various concentrations of tetracaine to be introduced over the surface in a buffer solution. Studies with membranes containing POPC (1-palmitoyl-2-oleoyl-*sn*-glycero-3-phosphocholine) yielded an equilibrium dissociation constant value of K_d = 180 ± 47 μm for this small molecule−membrane interaction. Adding cholesterol to the SLBs decreased the affinity between tetracaine and the bilayers, while this interaction tightened when POPE (1-hexadecanoyl-2-(9-*Z*-octadecenoyl)-*sn*-glycero-3-phosphoethanolamine) was added. Studies were also conducted with three negatively charged membrane lipids, POPG (1-palmitoyl-2-oleoyl-*sn*-glycero-3-phospho-(1′-*rac*-glycerol) (sodium salt)), POPS (1-palmitoyl-2-oleoyl-*sn*-glycero-3-phospho-L-serine (sodium salt)), and ganglioside GM1. All three measurements gave rise to a similar tightening of the apparent K_d value compared with pure POPC membranes. The lack of chemical specificity with the identity of the negatively charged lipid indicated that the tightening was largely electrostatic. Through a direct comparison with ITC measurements, it was found that the pH modulation sensor platform offers a facile, inexpensive, highly sensitive, and rapid method for the detection of interactions between putative drug candidates and lipid bilayers. As such, this technique may potentially be exploited as a screen for drug development and analysis.

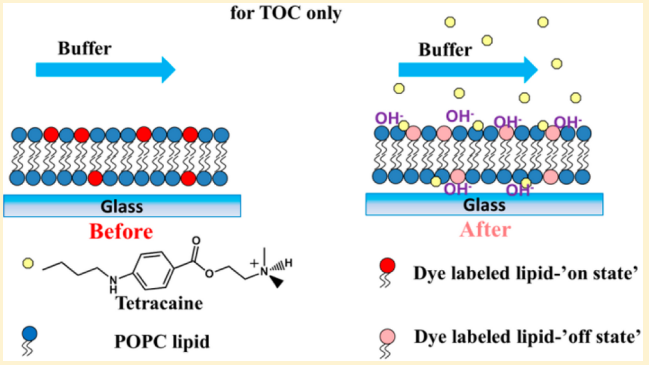

A great number of small drug molecules currently on the market target membrane-localized proteins, such as receptors and ion channels.[1,2] These molecules can also directly or indirectly interact with the surrounding lipid membrane,[3−6] which may lead to changes in a drug's function, properties, and availability.[7] Thus, it is important to understand the intrinsic interactions between drug molecules and lipid membranes. As most drugs are small molecules, whose properties may be altered greatly upon fluorescent labeling, it is imperative to employ label-free methods to study small molecule−membrane interactions. A number of techniques have been employed to detect these interactions including UV−vis spectroscopy,[8] nuclear magnetic resonance (NMR),[9−11] electron paramagnetic resonance (EPR),[12] quartz crystal microbalance with dissipation monitoring (QCM-D),[13] isothermal titration calorimetry (ITC),[14] vibrational spectroscopy (both infrared and Raman),[15−18] second harmonic generation (SHG) imaging,[7] ultraviolet−visible sum-frequency generation (UV−vis SFG),[19] differential scanning calorimetry (DSC),[20,21] and fluorescence spectroscopy based on a drug's intrinsic fluorescence.[22]

The methods enumerated above differ widely in their ease of use, signal-to-noise limits, expense, and requirements for technically trained operators. For example, QCM-D is relatively easy to use but has only modest sensitivity. Sensing based on a drug's intrinsic fluorescence may be quite useful in specific cases but is not universally suitable because of the limited fluorescence of many candidate molecules. On the other hand, SHG and UV−vis SFG are more universal techniques but require more sophisticated equipment and more advanced operator training. Moreover, NMR and EPR can potentially provide detailed molecular-level information but are of limited importance in high-throughput screening and have limited sensitivity. Raman and IR have better sensitivity but provide less chemically specific information and still are probably of only limited use in the development of screening assays. Perhaps the most widely accepted technique is ITC, which is often used to monitor drug molecule interactions with lipid

Received: June 28, 2013
Accepted: October 2, 2013
Published: October 23, 2013

vesicles in solution. Its sensitivity is limited by the degree of exothermicity of a given binding event, and studies with ITC require highly concentrated samples.

Herein, we will describe a new technique that uses much less lipid material, has higher throughput, and provides improved signal-to-noise compared with ITC. Moreover, this method works with supported lipid bilayers (SLBs),[23−25] which affords the ability to perform heterogeneous assays. This is a significant development because lipid vesicle solutions are employed in ITC in homogeneous assay formats, whereby drug molecules are constantly injected into continuously diluted samples. The advantage of heterogeneous assays with SLBs is that they can be run with a single lipid bilayer while the adjacent buffer solution is continuously replaced.[26−31] SLBs have been widely used as model cell membranes in vitro[32,33] and can have similar lipid compositions to cellular membranes as well as maintain the same two-dimensional fluidity.[24] Additionally, for studying drug−membrane interactions, it is advantageous to employ SLBs instead of liposomes, as SLBs require far less sample volume. Moreover, they can be integrated into an on-chip platform as part of a microfluidic device.

The strategy we wished to develop for detecting small molecule−membrane interactions is based on pH modulation sensing.[34−36] In the case of lipid membranes, this involves directly conjugating a pH sensitive dye such as *ortho*-Texas Red[34] or *ortho*-rhodamine B[36] to a phosphatidylethanolamine (PE) lipid embedded within a bilayer. These two dyes photobleach sufficiently slowly such that they suffer little, if any measurable degradation under the experimental conditions required to perform pH modulation studes.[34,36] Previously, we have shown that assays for target proteins can be developed when membrane-conjugated ligands are added to the membrane.[28,30] Upon binding of a target protein with a net charge, the interfacial potential is modulated, which in turn shifts the protonation state of the pH sensitive dye molecule. This strategy is extremely sensitive and can detect target protein concentrations in bulk solution, which are many orders of magnitude lower than the K_d value for the corresponding ligand−receptor binding event. As such, we reasoned that it should be possible to extend this idea to small molecule−membrane interactions in a heterogeneous assay, where QCM-D, SPR, or ITC have more difficulties due to intrinsic signal-to-noise limitations.

Herein, we demonstrate that the pH modulation approach can be exploited to monitor tetracaine−phospholipid interactions with outstanding sensitivity. Tetracaine is an anesthetic drug with a pK_a near 8.9 (molecular structure provided in Figure 1).[22,37,38] Its main activity is known to involve the blocking of ion channels in cell membranes. Extensive investigations of tetracaine−membrane interactions have been made over the last several decades. This includes the anesthetic mechanism for this drug,[39,40] its location within the lipid bilayer,[41,42] and the influence of the ionization state of tetracaine on its binding properties.[22] It has been reported that tetracaine inserts into biomembranes such that the butylamino group resides inside the lipid tale group region, while the protonated dimethylamino moiety is positioned near the phosphate moiety of the lipid headgroup.[42]

For the current experiments, 0.5 mol % *ortho*-rhodamine B-conjugated POPE (oRB−PE) was embedded in POPC bilayers to detect tetracaine (Figure 1). The experiments were performed at pH 7.1, where the drug bears a positive charge in bulk solution. Upon introducing the drug, a reversible

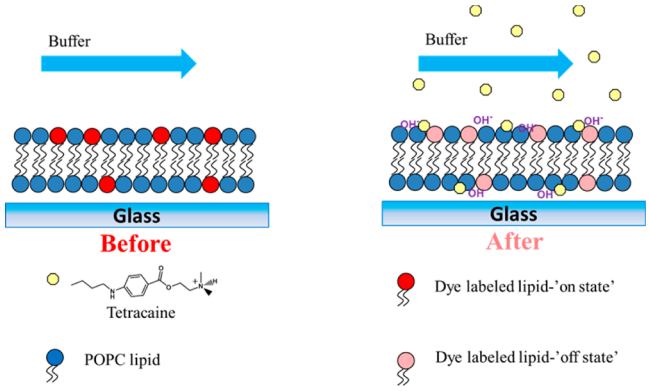

Figure 1. Schematic diagram illustrating the principles of oRB-PE acting as a reporter for drug-membrane binding. (Before) In the absence of the drug molecules, the fluorescent dyes are in the "on state", which is shown in in red. (After) Upon binding the drug molecules, the interfacial potential is increased, which recruits OH^- to the surface. As a result, the dye molecules in the lipid membrane are turned off (shown in pink).

decrease in the fluorescence response from oRB−PE was observed. This is consistent with the drug molecule making the interfacial potential more positively charged. By varying the drug concentration, it was possible to obtain a binding curve for the tetracaine/membrane interaction (K_d = 180 ± 47 μM). Moreover, it was found that this dissociation constant could be modulated by varying the lipid composition in the membrane.

EXPERIMENTAL SECTION

Materials. Lissamine rhodamine B sulfonyl chloride was purchased from Invitrogen (Eugene, OR). POPC, POPE, POPG, POPS, ganglioside GM1, and cholesterol were purchased from Avanti Polar Lipids (Alabaster, AL). Tetracaine came from Sigma-Aldrich (St. Louis, MO). The chemical structure of *ortho*-rhodamine B-POPE is shown in Figure 2a, and the structure of *ortho*-rhodamine B-conjugated-biotin (oRB−biotin, which is a soluble molecule) is shown in Figure 2b. The preparation of these molecules is described in the next section. Fibrinogen came from MP Biomedicals (Solon, OH). Purified water was obtained from a NANOpure Ultrapure Water System (18.2 MΩ·cm, Barnstead, Dubuque, IA). Glass coverslips (24 × 40 mm, No. 1.5) were purchased from Corning Inc. (Corning, NY). Microscope slides (25 × 75 × 1.0 mm) were from Fisher Scientific (Pittsburgh, PA), and PDMS (polydimethylsiloxane, Dow Corning Sylgard Silicone Elastomer-184) was obtained from Krayden, Inc. (El Paso, TX).

Rhodamine B-POPE and Rhodamine Biotin Preparation and Purification. Ten milligrams of rhodamine B sulfonyl chloride dissolved in 1 mL of anhydrous chloroform was added dropwise to 10 mg/mL of POPE in chloroform in an ice bath. After this, 2 μL of triethylamine was added to the mixed solution. The reaction was stirred for 4 h at room temperature. After the reaction, the mixture was spotted onto a TLC plate (EMD, 5715-7, silica gel 60 F254), blown dry with nitrogen gas, and developed with a chloroform−methanol mixture (92:8 by volume) to separate rhodamine-B labeled POPE mixed isomers from the reactants. The rhodamine B-POPE mixed isomers were then separated from each other on another TLC plate developed with a mixture of ammonium hydroxide solution, dichloromethane, and *n*-propanol (5:60:35 by volume). Each separated band on the TLC plate was

dx.doi.org/10.1021/ac401955t | *Anal. Chem.* 2013, 85, 10240−10248

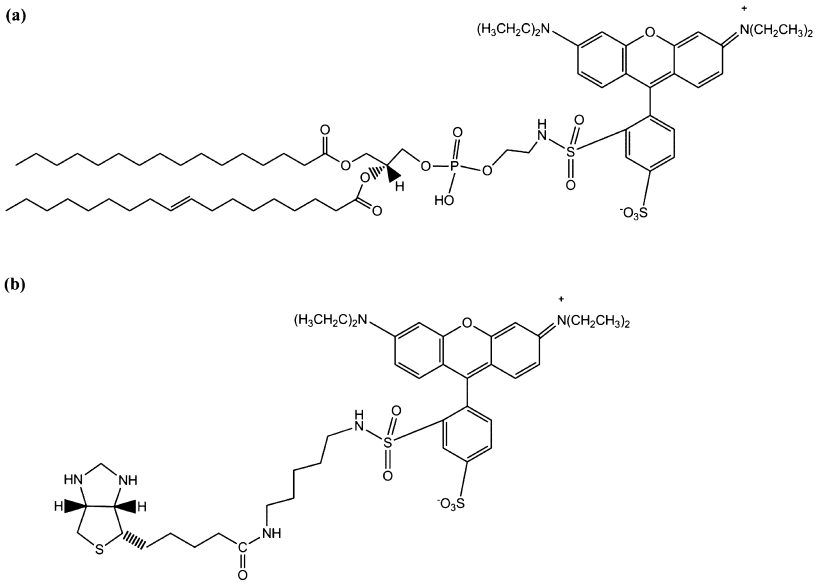

Figure 2. Structures of (a) oRB−PE and (b) oRB−biotin.

scratched off with a razor blade and collected onto a column. A mixture of chloroform and methanol (7:3 by volume) was utilized to elute the dye-conjugated lipids from the surface. The concentration of each isomer of rhodamine B-conjugated POPE was measured by UV−vis.

The preparation and purification of the oRB−biotin conjugate was done in a manner analogous to the preparation of oRB−POPE. In this case, 5 mg/mL pentylamine−biotin (Fisher Scientific, Pittsburgh, PA) was used instead of POPE.

Small Unilamellar Vesicles (SUVs) Preparation. Lipids were mixed at the desired mole ratio in chloroform in a glass vial. Afterward, the chloroform was removed by continuous purging with nitrogen. Desiccation was then performed under vacuum for more than 2 h to remove any residual organic solvent. The dried lipid films were hydrated with 10 mM phosphate-buffered saline (PBS) containing 150 mM NaCl, followed by sonication in a bath to obtain 0.5 mg/mL lipid suspensions. These suspensions were then subjected to at least seven freeze−thaw cycles with liquid nitrogen and water (room temperature) and at least seven extrusion cycles through two stacked 100 nm polycarbonate membranes (Whatman) using a Lipex extruder (Northern Lipids, Inc., Vancouver, Canada). The size of the lipid vesicles was about 95 ± 10 nm as determined by dynamic light scattering measurements (Brookhaven Instruments 90Plus Particle Size Analyzer). The nascently prepared SUV solutions were stored at 4 °C until use.

Flow Cell Fabrication. A flow cell setup was employed to introduce drug molecules above a supported lipid bilayer on a glass slide (Figure 3). A polydimethylsiloxane (PDMS) cover block served as the ceiling of the device. Two small holes in this block served as inlet and outlet ports for flowing liquid. The flow of analyte solution into and out of the device was driven by gravity, and the rate of flow was controlled by the size of the outlet hole.

The PDMS block was placed directly over a second thin PDMS film (0.52−0.64 mm) with an 8 mm diameter hole in the middle that defined the exposed area of a No. 2 glass coverslip placed beneath it. Flowing aqueous solutions came into contact with this exposed area. Two thin stainless steel

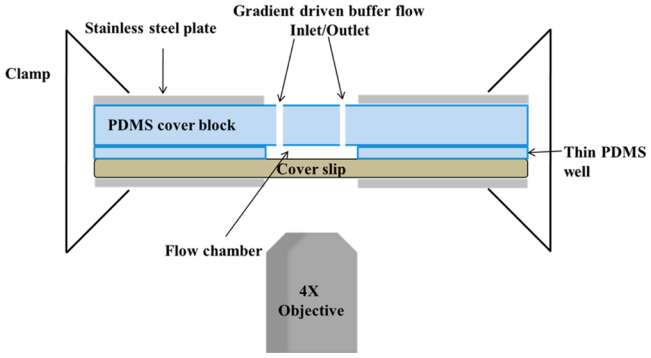

Figure 3. Side view of the flow cell. PDMS cover block, PDMS well, and coverslip fit snugly between the two stainless steel plates. SLB is coated on the top side of the coverslip. Drawing is not to scale.

plates (6.5 cm × 3.0 cm) with a 1.0 cm diameter hole in the center clamped the entire flow cell together.

PDMS Stamp and Patterned SLBs. After placing the thin PDMS film on a coverslip surface, lipid bilayers were patterned in stripes onto the glass inside the circular PDMS hole. Such patterning provided a simple method for comparing signal changes in the SLBs with the background fluorescence intensity during an experiment. To do this, a PDMS stamp was formed by curing initially un-cross-linked PDMS overnight over a patterned glass mold at room temperature.[43] The glass mold had a series of 380 μm × 1 cm parallel lines spaced 200 μm from each other that were fabricated by HF etching.[44] The PDMS stamp was then cut into appropriately sized sections that would just fit inside the PDMS well in the flow cell. Once cured, the molds were soaked overnight in hexane to remove any uncured PDMS. They were then dried at room temperature and rinsed with ethanol and purified water.

To obtain patterned SLBs, the PDMS stamps were put into conformal contact with the glass surface in the flow cell and fixed in place with a piece of tape. Next, a 1 mg/mL fibrinogen solution was injected into the well and incubated for 5 min, forming a fibrinogen monolayer on the uncovered portions of the glass. The fibrinogen solution was washed away in a 150 mM NaCl solution before the PDMS stamp was peeled off.

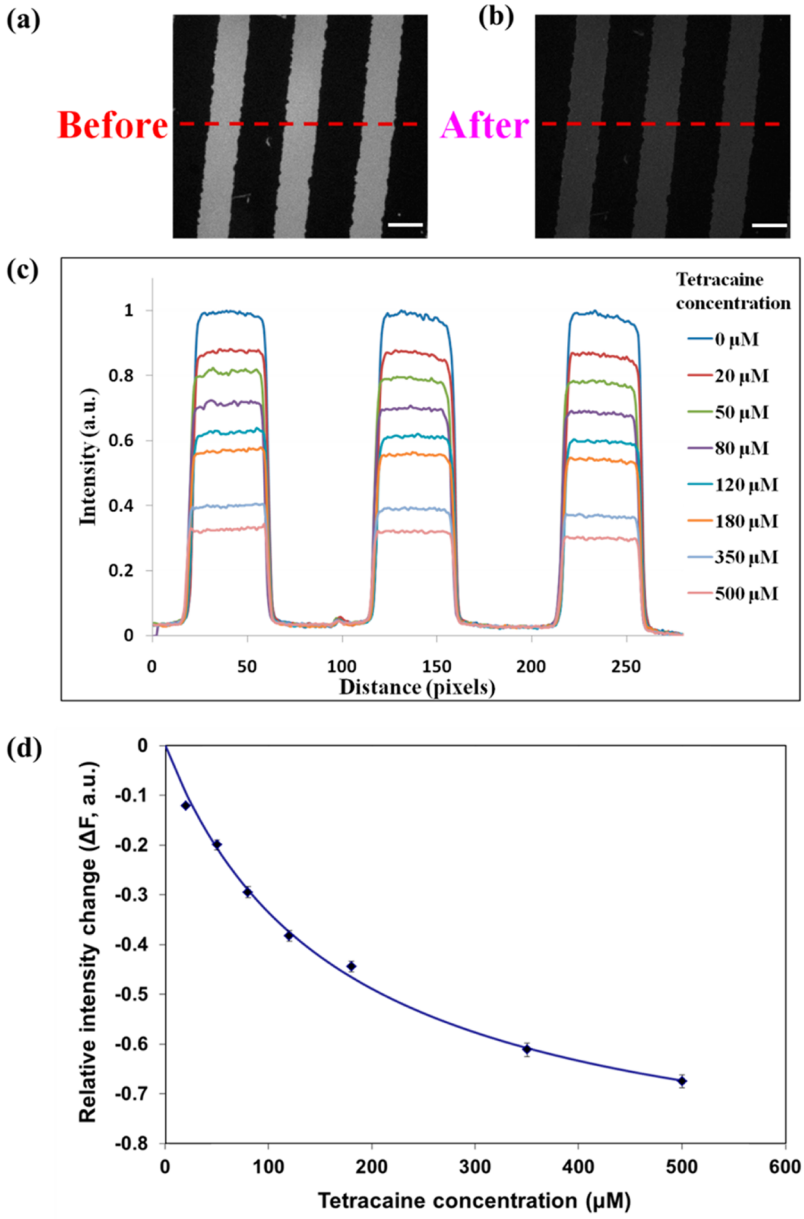

Figure 4. Sensing tetracaine–POPC bilayer interactions. Epifluorescence images of a stripped bilayer pattern in a flow cell (a) before and (b) after the introduction of 500 μM tetracaine. Scale bars shown in white are 1 mm. (c) Line scan profiles for the same patterned bilayer under bulk tetracaine concentrations ranging from 0 to 500 μM. Red dashed lines in (a) and (b) represent the regions used obtain the line scans. (d) Plot of the relative fluorescence intensity change vs bulk tetracaine concentration. The blue solid line is the best fit to a Langmuir isotherm for these data points.

Finally, the desired lipid vesicle solution was introduced into the well. This caused a one-layer thick supported lipid bilayer to form by vesicle fusion to the portions of the glass support that were not blocked by the protein monolayer.[25,45] After this, the PDMS block was introduced so that drug solutions could flow into the chamber.

It should be noted that all glass coverslips employed for bilayer formation were first cleaned in a near-boiling mixture of ICN 7X detergent (Costa Mesa, CA) and purified water (1:4 volume ratio), followed by rinsing the coverslips sequentially with purified water and ethanol at least three times. The coverslips were then dried under flowing nitrogen and annealed at 530 °C for 5 h in a kiln (Sentry Xpress 2.0, Orton Ceramic Foundation, OH), which render the surface of the glass both smooth and hydrophilic. Also, the thin PDMS film used in the flow cell was fabricated by curing PDMS between two silanized glass plates with a spacer of four stacked No. 1 coverslips (100–150 μm thick) and trimmed to the correct size to fit the flow cell. A round section was cut out to form the well. The thicker PDMS cover block was made the same way except that a 4 mm thick spacer was used instead. Two holes were reamed into this block by the tip of a hollow needle.

pH Titration Curves. Experiments were performed to obtain titration curve data for 0.5 mol % *ortho*-rhodamine B-POPE in POPC bilayers as well as with bilayers containing 20 mol % POPE, 20 mol % cholesterol, and 20 mol % POPS (Figure S1). The pH of the bulk solution above the bilayers was altered via the continuous flow of 50 mM phosphate solutions adjusted by NaOH or NaCl to the corresponding pH value. The fluorescence intensity of the bilayer was monitored until steady state was achieved. A pH value of 7.1 was selected for the tetracaine detection measurements described below because

dx.doi.org/10.1021/ac401955t | *Anal. Chem.* 2013, 85, 10240–10248

it falls within the pH responsive range of the dye-conjugated lipid.

Fluorescence Microscopy. A Nikon Eclipse Ti−U fluorescence microscope (Tokyo, Japan) equipped with a ProEM 1024 CCD camera (Princeton Instruments) and Lumen 200 (Prior Scientific) light source was utilized to take fluorescence images. Both 4X and 10X air objectives (N.A. = 0.13 and 0.30, respectively) were used for imaging along with a Texas Red filter set (Chroma Technology, Bellows Falls, VT). Exposure times were kept to an absolute minimum to minimize photobleaching (always less than 200 ms/exposure). As such, appreciable photobleaching could not be discerned within error for these measurements. MetaMorph software (Version 7.7.0.0, Universal Imaging) was employed to process the images.

RESULTS AND DISCUSSION

Sensing Tetracaine/POPC-Supported Bilayer Interactions. SLBs containing 99.5 mol % POPC and 0.5 mol % oRB−PE were utilized for sensing tetracaine−membrane interactions in an initial series of experiments. This work was performed with 50 mM sodium phosphate buffer at pH 7.1 ± 0.1.[36] The buffer was circulated over the patterned bilayers until fluorescence stabilization was achieved (Figure 4a). Next, tetracaine at concentrations ranging from 0 to 500 μM was introduced into the buffer and continuously flowed through the flow cell until the fluorescence intensity from the lipid bilayer stabilized. Images were captured every 5 min and stabilization took about 30 min at the lowest drug concentration. It should be noted that the time it took to achieve equilibrium was controlled by the dead volume of flow cell, which was ∼250 μL. Specifically, it took ∼15 min to completely replace the solution at a flow rate of 1 mL/hour. A representative image after equilibration with 500 μM tetracaine is shown in Figure 4b. The individual fluorescence line scans for eight tetracaine concentrations are shown in Figure 4c. As can be seen, the fluorescence intensity of the lipid bilayer decreased with increasing concentration of the drug molecule. At the highest concentration of tetracaine employed, 500 μM, the fluorescence intensity decreased by more than a factor of 3. With removal of the drug molecule, the fluorescence reverted back to the starting intensity, and hence, the whole process was completely reversible (Figure S5). This indicates that tetracaine could be completely removed from the membrane. The data in Figure 4c represent a signal-to-noise ratio of ∼400:1. This corresponds to a detection limit of about 3 μM at the 99% confidence level.

Using the data from Figure 4c, the relative fluorescence intensity decrease could be plotted as a function of drug molecule concentration (Figure 4d). The y-axis represents the relative fluorescence change ΔF, which is calculated as $(F-_0)/F_0$, which reduces to F/F_0-1. In this equation, F is the fluorescence intensity of the bilayer as a function of tetracaine concentration in the bulk solution, whereas F_0 is the fluorescence intensity of the bilayer in pure buffer.

The data in Figure 4d can be fit to a Langmuir isotherm as shown by the blue solid line. The apparent equilibrium dissociation constant is abstracted using (eq 1):

$$\Delta F = -a\frac{[T]}{K_d + [T]} \quad (1)$$

where T is the bulk concentration of tetracaine and a is a constant corresponding to the maximum relative fluorescence intensity change. The fit yields a K_d of 180 ± 47 μM, which is consistent with the literature value for this binding event found by nonlinear optical measurements.[7] As a control experiment, the direct interaction of tetracaine with the dye molecule was probed in bulk solution in a QVFL-Q-10 cuvette within a QE 65000-FL scientific grade spectrometer. In this case, 1 μM *ortho*-rhodamine B-conjugated biotin was placed in a 50 mM sodium phosphate buffer solution (pH 7.1 ± 0.1). Solution conditions were varied to consist of up to 1 mM tetracaine. No changes in the fluorescence intensity were noted within experimental error, even at the highest concentration of the drug molecule.

It should be noted that although the detection limit was 3 μM for the experiments in Figure 4, this value could easily be lowered by several orders of magnitude by simply averaging the data over the entire sample area, making multiple measurements as a function of time, or decreasing the buffer concentration by analogy with work done for protein−membrane interactions.[34,36] For example, by utilizing a 10X objective and 0.5 mM sodium phosphate buffer solution (pH 7.1 ± 0.1), it was easily possible to detect 25 pM tetracaine (Figure 5) with a detection limit of ∼10 pM. This measurement

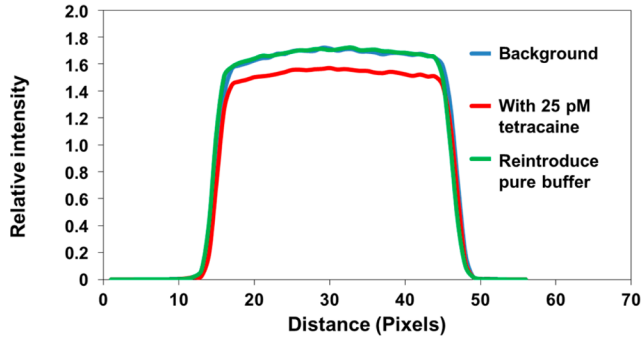

Figure 5. Fluorescence intensity line scan of a POPC SLB with 0.5 mM sodium phosphate buffer (pH 7.1 ± 0.1) without tetracaine (blue and green) and with 25 pM tetracaine (red).

was also completely reversible after the reintroduction of pure buffer. The reason for the improved detection limit under these conditions was partially due to the higher light gathering power of the 10X objective (N.A. = 0.30 versus only NA = 0.13 for the 4X objective). Moreover, the decrease in the ionic strength of the solution led to an increase in the Debye length. This, in turn, allowed more distant fluorophores to be effected by tetracaine binding under otherwise similar experimental conditions.[17] An even lower detection limit could be achieved by further decreasing the ionic strength. Specifically, a detection limit of ∼1 pM tetracaine (Figure S6) could be achieved by working at 5 μM sodium phosphate (pH 7.1 ± 0.1). This corresponds to a limit of detection 7 orders of magnitude smaller than the K_d value. However, the buffering capacity of the solution is eroded as the buffer concentration is lowered. Therefore, there is a trade-off between the limit of detection and maintaining a stable pH value. In fact, the 5 μM buffer seemed to represent a practical limit for maintaining a steady fluorescence signal.

Effect of Cholesterol on Tetracaine−Bilayer Binding. In a next set of experiments, cholesterol was introduced to POPC SLBs with 0.5 mol % oRB−PE and tested for tetracaine interactions. Cholesterol, an important constituent in mammalian cells, varies significantly in concentration in the membranes of various organelles.[46,47] It influences cell membranes via its

interactions with lipids and membrane-associated proteins.[48] Herein, cholesterol concentrations were varied from 0 to 45 mol %. The assays were otherwise carried out under the same conditions as those in Figure 4. Fluorescence modulation assays were performed with five different cholesterol concentrations (Figure 6a), and the values for K_d as a function of cholesterol

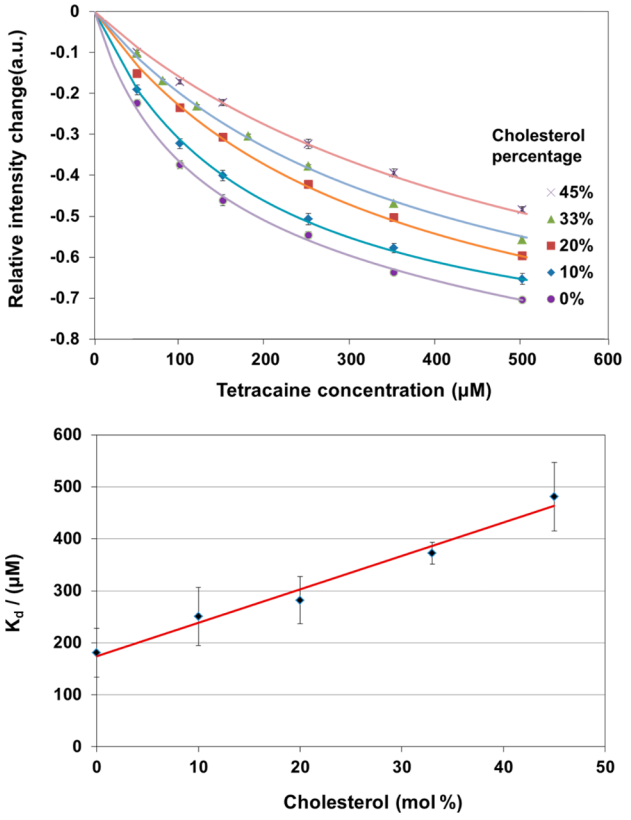

Figure 6. Tetracaine–POPC bilayer interactions as a function of cholesterol. (a) Plots of relative fluorescence intensity change vs bulk tetracaine concentration for five different cholesterol concentrations: 0, 10, 20, 33, and 45 mol %. Solid lines are the best fits to Langmuir isotherms. (b) Plot of K_d vs cholesterol concentration from the data in (a). The red solid line represents the best linear fit to the data.

are plotted in Figure 6b. As can be seen, K_d weakened approximately 3-fold and did so in a linear fashion with increasing cholesterol concentration. This attenuation in the strength of the tetracaine–bilayer interaction is in agreement with previous reports. Specifically, Zhang and co-workers found that 28 mol % cholesterol in DPPC bilayers decreased the partition coefficient of tetracaine to the bilayer both below and above its phase transition temperature.[22] Nguyen et al. have shown that a decrease in tetracaine binding to SOPC, DMPC, and DPPC bilayers could be observed after incorporating 28 mol % cholesterol.[7] Both of these previous studies were, however, performed at just this single concentration of cholesterol. Our current data showing a linear weakening of the K_d value with the mol % cholesterol in a POPC bilayer is consistent with the notion that cholesterol increases the packing density of the lipids in the bilayer and leaves less room for the small molecule to insert.[7] In fact, according to Kim et al., the mean headgroup area per DPPC molecule should decrease linearly with increasing cholesterol concentration.[49]

Effect of POPE on Tetracaine–Bilayer Binding. Phosphatidylethanolamine (PE) is composed of a glycerol moiety that is esterified with two fatty acids and a phosphate group. The negatively charged phosphate group is conjugated to a positively charged ethanolamine group, which makes the whole molecule zwitterionic at pH 7.1 ± 0.1. PE usually constitutes 20–50% of the total phospholipid content in mammalian cells, which makes it the second most abundant lipid after phosphotidylcholine (PC).[50] Thus, it is important to discern the influence of PE on tetracaine/membrane interactions. For the current studies, POPE was chosen as a model PE lipid because it has the same tale groups as POPC. It should be noted that PE is more basic than PC with pK_a = ~9.6 for the amino group.[51]

To test the influence of POPE on tetracaine–bilayer interactions, up to 20 mol % POPE was incorporated into POPC SLBs. This upper concentration limit was chosen because greater PE concentrations may impede vesicle fusion to the planar glass supports.[52] Binding curve data are provided in Figure S-2 in the Supporting Information section, and the extracted apparent K_d values are plotted in Figure 7. As can be

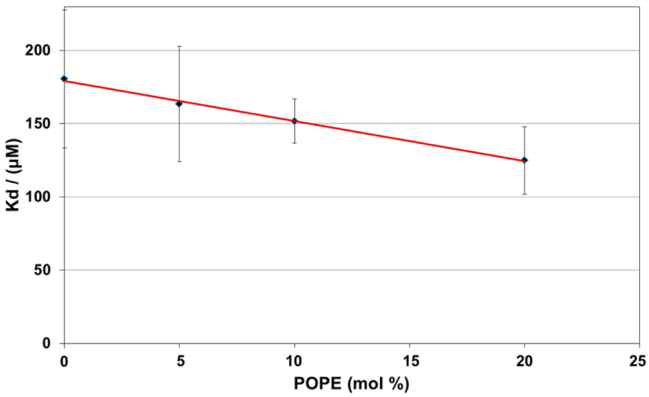

Figure 7. Plot of the K_d value for tetracaine vs the POPE concentration in POPC membranes. The red solid line represents a linear fit to the data.

seen, PE had the opposite effect of cholesterol. Specifically, the K_d value for tetracaine binding tightened from 180 ± 47 μM to 124 ± 23 μM when 20 mol % POPE was added to the SLBs. Once again, the trend appeared to be linear with the added lipid component.

The linear increase of tetracaine affinity with increasing POPE concentration may be related to hydrogen bonding between POPE lipids and tetracaine. Several studies have demonstrated the ability of PE to hydrogen bond with various small molecules.[53−56] Herrera et al. demonstrated that there are hydrogen bonds formed between an amino acid's carboxylate group and the R–NH_3^+ from PE when arginine interacts with the DMPE bilayer. Moreover, the carbonyl moiety of PE lipid is able to hydrogen bond with the guanidinium moiety of arginine.[53] Pink et al. have proposed hydrogen bond formation between PC and PE, which would need to form between either the NH_3^+ and PO_2^- or NH_3^+ and C=O.[55] By analogy, a hydrogen bond is likely to form between the R–NH_3^+ group on POPE and the C=O group on tetracaine.

It has been observed that the incorporation of PE into phospholipid bilayers reduces interchain hydration while enhancing headgroup hydration.[57] However, because PE lipids have a relatively small and cone-shaped headgroup, it is

dx.doi.org/10.1021/ac401955t | Anal. Chem. 2013, 85, 10240−10248

energetically unfavorable to have an increase in headgroup hydration, which makes planar bilayers unstable.[58,59] Evidence from a ^{31}P NMR study has shown that tetracaine inserts into PE-containing bilayers by acting as a wedge, which helps stabilize the membrane.[60] As such, the relatively stronger affinity between tetracaine and POPE-containing bilayers may be the result of relieving the lipid packing constraints caused by the presence of POPE.

Effect of Negatively Charged Lipids on Tetracaine−Bilayer Binding. In addition to uncharged and zwitterionic components, there are also negatively charged lipids in bilayers such as phosphatidylserine (PS), phosphatidylglycerol (PG), and gangliosides. Although they are not as abundant in biological membranes as PE or cholesterol, negatively charged lipids are tightly regulated and play a key role in membrane chemistry.[61−66] Moreover, these components should interact at least electrostatically with the positively charged tetracaine.

Experiments were carried out with POPG, POPS, and GM1 using nearly the same conditions and procedures as described above. The buffer for POPG and GM1-containing SLBs was 50 mM sodium phosphate (pH 7.1 ± 0.1), while the buffer with POPS also contained 0.8 mM EDTA due to the potential quenching ability of trace concentrations of divalent metal ions such as Cu^{2+}.[67] The apparent dissociation constant for tetracaine as a function of each negatively charged lipid components are provided in Figure 8. The associated binding

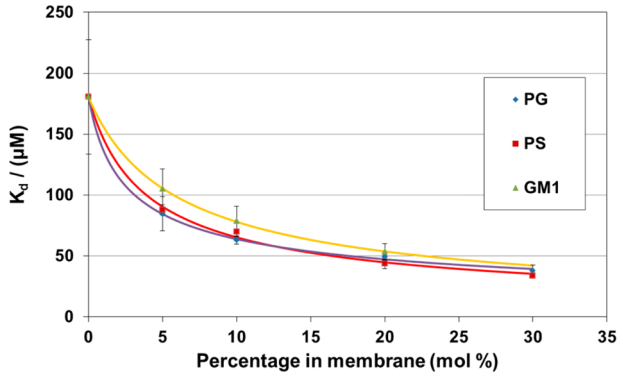

Figure 8. Plot of the K_d values for tetracaine vs the mol % of negatively charged lipids for PG (blue diamond), PS (red square), and ganglioside GM1 (green triangle). The solid curves represent the best curve fit to the data.

curve data are provided in the Supporting Information section in Figure S-3. It should be noted that data at 30 mol % is only provided for POPG and POPS as vesicles containing 30 mol % GM1 would not easily form supported bilayers.

As can be seen from Figure 8, the influence of POPS, POPG, and GM1 on the K_d values is essentially identical. Thus, the effect should be simply electrostatic rather than chemically specific. Indeed, the incorporation of any of these three molecules into the bilayer will make the surface potential more negative.[68] This, in turn, will enhance the electrostatic interactions between the bilayer and the positively charged tetracaine molecules. Moreover, the presence of negatively charged lipids leads to a tightening of the dissociation constant only at lower concentrations of the negatively charged lipid, while this effect flattens out as the concentration is increased further. This finding is consistent with the idea that the surface potential decreases nonlinearly as additional negatively charged lipids are introduced into the membrane.[68] The overall effect is to tighten the dissociation constant by approximately a factor of 6 when 30 mol % of a given negatively charged lipid is present (Figure 8).

Comparison with ITC. As noted in the introduction, a variety of methods have been employed to investigate the interactions of membranes with small molecules.[8−22] As ITC is probably the most commonly employed of these techniques, we wished to benchmark the current pH modulation results against it. To do this, ITC measurements were performed with a MicroCal Auto-iTC200 (Pittsburgh, PA) using nearly the same tetracaine−POPC binding conditions described in Figure 4. However, since measurements could not be made with supported bilayers, 100 nm diameter POPC vesicles (0.76 mg/mL) in 50 mM sodium phosphate buffer (pH 7.1 ± 0.1) were used instead. In order to obtain a binding curve, 1.5 μL of 10 mM tetracaine aliquots was introduced into 370 μL of the vesicle solution in 25 separate injections. A K_d value of 126 ± 65 μM was found for this interaction, and the detection limit was ∼1 μM. Experiments were also run with POPC vesicles containing 0.5 mol % oRB−PE. In this case, we found K_d = 103 ± 53 μM. The raw ITC data and curve fits are provided in Figure S-4 of the Supporting Information section. Within experimental error, both of these measurements are the same and agree well with the data from Figure 4, where a value of 180 ± 47 μM for K_d was found. Such ITC measurements serve as an additional control to verify that adding 0.5 mol % oRB−PE as a probe in the pH modulation assays had little if any effect on the experiment. It should be noted that there could be a small difference in the K_d values between the ITC and pH modulation experiments since the former was done with vesicles and thus have curved surfaces, whereas the supported membranes are essentially flat. Apparently, any such binding differences caused by this degree of curvature do not lead to significant differences within experimental error.

There are significant advantages to making drug−membrane interaction measurements by the pH modulation technique compared with ITC. These include the relatively small sample sizes required in the former case. In fact, in order to obtain an acceptable signal from ITC, 400 μL of a 0.76 mg/mL vesicle solution must be prepared. Moreover, 1.5 μL of highly concentrated (10 mM) tetracaine aliquots were introduced into the vesicle solution in 25 separate injections. By comparison, the amount of lipid material required in the pH modulation setup was several orders of magnitudes less. It should be noted that the pH modulation experiments can also be run in microfluidic channels, where only a few microliters of bulk sample would flow, although that was not done here. Smaller lipid and drug sample volumes would represent a significant advantage when exploring the interactions of expensive or rare drug molecules with membranes. Second, the pH modulation assay can be run under conditions where the detection limit of the assays outstrips ITC by at least 4 or 5 orders of magnitude (Figure 5). Third, the cost of a typical ITC instrument is over $100,000, while fluorescence measurements can be made with a setup costing much less than this. Finally, the current fluorescence-based technique has the potential for easy multiplexing by employing patterned bilayer membranes to explore multiple membrane interactions at once.[69,70] In fact, dozens, if not hundreds of interactions could be explored simultaneously. Such multiplexing advantages would be much more difficult to realize by ITC measurements.

It should be noted that there are also inherent advantages of ITC. For example, this technique directly measures heat

transfer, which affords the most straightforward way to obtain ΔH values for the drug−membrane interactions. One could also image circumstances under which a particular drug might directly interact with the dye molecule employed as the probe in the pH modulation sensing assay. Finally, it should be noted that both methods provide thermodynamic information and can thus benefit from complementary spectroscopy measurements such as FTIR, Raman, or NMR to provide molecular level details concerning drug−membrane interactions.

CONCLUSION

As demonstrated above, our pH modulation sensor platform can be employed to measure K_d values for the interactions of tetracaine with phospholipid membranes. This assay could easily be applied to study the membrane interactions of other small drug molecules such as ibuprofen, aspirin, and saxagliptin.[71−73] Drug−membrane binding should arise largely from van der Waals, hydrophobic, packing, hydrogen bonding, and electrostatic interactions.[22,42,53] The K_d value measured for the interaction of tetracaine with supported POPC bilayers was 180 ± 47 μM. This value could be modestly weakened by adding cholesterol to the membrane (K_d = 350 μM with 33 mol % cholesterol) or modestly tightened by adding POPE or negatively charged lipids to the membrane (K_d = 35 μM with 30 mol % DOPG). Each set of measurements could be made within a few minutes. Also, the surface area covered by the lipid bilayer involved less than 10^{15} lipid molecules, since the surface coverage inside the flow device was under 1 cm^2. This platform offers a facile and rapid method for the detection of interactions between drug molecules and lipid bilayers, especially when compared with ITC. Thus, it may be developed into a rapid screening assay and used in a multiplexed format to detect interactions with many different types of lipid membranes simultaneously.

ASSOCIATED CONTENT

Supporting Information

Additional figures and experimental details including pH titration curves, binding curves as a function of POPE, GM1, POPS, and POPG concentration, ITC data, experimental reversibility tests, and low concentration tetracaine experiments. This material is available free of charge via the Internet at http://pubs.acs.org.

AUTHOR INFORMATION

Corresponding Author

*E-mail: psc11@psu.edu.

Notes

The authors declare no competing financial interest.

ACKNOWLEDGMENTS

This work was funded by a grant from the Office of Naval Research (N00014-08-1-0467).

REFERENCES

(1) McNeely, P. M.; Naranjo, A. N.; Robinson, A. S. *Biotechnol. J.* **2012**, *7*, 1451−1461.
(2) Rask-Andersen, M.; Almen, M. S.; Schioth, H. B. *Nat. Rev. Drug. Discov.* **2011**, *10*, 579−590.
(3) Austin, R. P.; Barton, P.; Davis, A. M.; Fessey, R. E.; Wenlock, M. C. *Pharm. Res.* **2005**, *22*, 1649−1657.
(4) Fisar, Z.; Fuksova, K.; Velenovska, M. *Gen. Physiol. Biophys.* **2004**, *23*, 77−99.
(5) Howell, B. A.; Chauhan, A. *Langmuir* **2009**, *25*, 12056−12065.
(6) Pajeva, I. K.; Wiese, M.; Cordes, H. P.; Seydel, J. K. *J. Cancer Res. Clin. Oncol.* **1996**, *122*, 27−40.
(7) Nguyen, T. T.; Conboy, J. C. *Anal. Chem.* **2011**, *83*, 5979−5988.
(8) Custodio, J. B. A.; Almeida, L. M.; Madeira, V. M. C. *Biochem. Biophys. Res. Commun.* **1991**, *176*, 1079−1085.
(9) Auger, M.; Jarrell, H. C.; Smith, I. C. P. *Biochemistry* **1988**, *27*, 4660−4667.
(10) Peng, X. D.; Jonas, A.; Jonas, J. *Chem. Phys. Lipids* **1995**, *75*, 59−69.
(11) Castro, V.; Stevensson, B.; Dvinskikh, S. V.; Hogberg, C. J.; Lyubartsev, A. P.; Zimmermann, H.; Sandstrom, D.; Maliniak, A. *Biochim. Biophys. Acta, Biomembr.* **2008**, *1778*, 2604−2611.
(12) De Paula, E.; Schreier, S. *Biochim. Biophys. Acta, Biomembr.* **1995**, *1240*, 25−33.
(13) Paiva, J. G.; Paradiso, P.; Serro, A. P.; Fernandes, A.; Saramago, B. *Colloids Surf., B* **2012**, *95*, 65−74.
(14) Moreno, M. M.; Garidel, P.; Suwalsky, M.; Howe, J.; Brandenburg, K. *Biochim. Biophys. Acta, Biomembr.* **2009**, *1788*, 1296−1303.
(15) Shibata, A.; Ikawa, K.; Terada, H. *Biophys. J.* **1995**, *69*, 470−477.
(16) Auger, M.; Smith, I. C. P.; Mantsch, H. H.; Wong, P. T. T. *Biochemistry* **1990**, *29*, 2008−2015.
(17) Fox, C. B.; Harris, J. M. *J. Raman. Spectrosc.* **2010**, *41*, 498−507.
(18) Fox, C. B.; Horton, R. A.; Harris, J. M. *Anal. Chem.* **2006**, *78*, 4918−4924.
(19) Nguyen, T. T.; Rembert, K.; Conboy, J. C. *J. Am. Chem. Soc.* **2009**, *131*, 1401−1403.
(20) Tokarska-Schlattner, M.; Epand, R. F.; Meiler, F.; Zandomeneghi, G.; Neumann, D.; Widmer, H. R.; Meier, B. H.; Epand, R. M.; Saks, V.; Wallimann, T.; Schlattner, U. *PLoS One* **2012**, *7*, 1−11.
(21) Lucio, M.; Bringezu, F.; Reis, S.; Lima, J. L. F. C.; Brezesinski, G. *Langmuir* **2008**, *24*, 4132−4139.
(22) Zhang, J. Z.; Hadlock, T.; Gent, A.; Strichartz, G. R. *Biophys. J.* **2007**, *92*, 3988−4001.
(23) Sackmann, E. *Science* **1996**, *271*, 43−48.
(24) Cremer, P. S.; Boxer, S. G. *J. Phys. Chem. B* **1999**, *103*, 2554−2559.
(25) Castellana, E. T.; Cremer, P. S. *Surf. Sci. Rep.* **2006**, *61*, 429−444.
(26) Liu, Y.; Liao, P.; Cheng, Q.; Hooley, R. J. *J. Am. Chem. Soc.* **2010**, *132*, 10383−10390.
(27) Kissler, S.; Pierrat, S.; Zimmermann, T.; Vogt, H.; Trieu, H. K.; Koper, I. *Biomed. Tech.* **2012**, *57*, 1010−1013.
(28) Benkoski, J. J.; Jesorka, A.; Kasemo, B.; Hook, F. *Macromolecules* **2005**, *38*, 3852−3860.
(29) Joubert, J. R.; Smith, K. A.; Johnson, E.; Keogh, J. P.; Wysocki, V. H.; Gale, B. K.; Conboy, J. C.; Saavedra, S. S. *ACS Appl. Mater. Interfaces* **2009**, *1*, 1310−1315.
(30) Forstner, M. B.; Yee, C. K.; Parikh, A. N.; Groves, J. T. *J. Am. Chem. Soc.* **2006**, *128*, 15221−15227.
(31) Szmodis, A. W.; Blanchette, C. D.; Longo, M. L.; Orme, C. A.; Parikh, A. N. *Biointerphases* **2010**, *5*, 120−130.
(32) Dewa, T.; Sugiura, R.; Suemori, Y.; Sugimoto, M.; Takeuchi, T.; Hiro, A.; Iida, K.; Gardiner, A. T.; Cogdell, R. J.; Nango, M. *Langmuir* **2006**, *22*, 5412−5418.
(33) Tero, R.; Ujihara, T.; Urisut, T. *Langmuir* **2008**, *24*, 11567−11576.
(34) Jung, H.; Robison, A. D.; Cremer, P. S. *J. Am. Chem. Soc.* **2009**, *131*, 1006−1014.
(35) Huang, D.; Robison, A. D.; Liu, Y. Q.; Cremer, P. S. *Biosens. Bioelectron.* **2012**, *38*, 74−78.
(36) Robison, A. D.; Huang, D.; Jung, H.; Cremer, P. S. *Biointerphases* **2013**, *8*, 1−9.
(37) Fodor, A. A.; Gordon, S. E.; Zagotta, W. N. *J. Gen. Physiol.* **1997**, *109*, 3−14.
(38) Roth, S. H. *Annu. Rev. Pharmacol. Toxicol.* **1979**, *19*, 159−178.
(39) Lee, A. G. *Nature* **1976**, *262*, 545−548.

(40) Weizenmann, N.; Huster, D.; Scheidt, H. A. *Biochim. Biophys. Acta, Biomembr.* **2012**, *1818*, 3010−3018.
(41) Hutterer, R.; Kramer, K.; Schneider, F. W.; Hof, M. *Chem. Phys. Lipids* **1997**, *90*, 11−23.
(42) Kuroda, Y.; Fujiwara, Y. *Biochim. Biophys. Acta* **1987**, *903*, 395−410.
(43) Liu, C. M.; Monson, C. F.; Yang, T. L.; Pace, H.; Cremer, P. S. *Anal. Chem.* **2011**, *83*, 7876−7880.
(44) Holden, M. A.; Kumar, S.; Beskok, A.; Cremer, P. S. *J. Micromech. Microeng.* **2003**, *13*, 412−418.
(45) Brian, A. A.; McConnell, H. M. *Proc. Natl. Acad. Sci. U.S.A.* **1984**, *81*, 6159−6163.
(46) Cansell, M.; Gouygou, J. P.; Jozefonvicz, J.; Letourneur, D. *Lipids* **1997**, *32*, 39−44.
(47) Corvera, S.; DiBonaventura, C.; Shpetner, H. S. *J. Biol. Chem.* **2000**, *275*, 31414−31421.
(48) Ikonen, E. *Nat. Rev. Mol. Cell Biol.* **2008**, *9*, 125−138.
(49) Kim, K.; Kim, C.; Byun, Y. *Langmuir* **2001**, *17*, 5066−5070.
(50) Vance, J. E. *J. Lipid Res.* **2008**, *49*, 1377−1387.
(51) Tsui, F. C.; Ojcius, D. M.; Hubbell, W. L. *Biophys. J.* **1986**, *49*, 459−468.
(52) Hamai, C.; Yang, T. L.; Kataoka, S.; Cremer, P. S.; Musser, S. M. *Biophys. J.* **2006**, *90*, 1241−1248.
(53) Herrera, F. E.; Bouchet, A.; Lairion, F.; Disalvo, E. A.; Pantano, S. *J. Phys. Chem. B* **2012**, *116*, 4476−4483.
(54) Nussio, M. R.; Voelcker, N. H.; Sykes, M. J.; McInnes, S. J. P.; Gibson, C. T.; Lowe, R. D.; Miners, J. O.; Shapter, J. G. *Biointerphases* **2008**, *3*, 96−104.
(55) Pink, D. A.; McNeil, S.; Quinn, B.; Zuckermann, M. J. *Biochim. Biophys. Acta, Biomembr.* **1998**, *1368*, 289−305.
(56) Sen, A.; Yang, P. W.; Mantsch, H. H.; Hui, S. W. *Chem. Phys. Lipids* **1988**, *47*, 109−116.
(57) Ho, C.; Slater, S. J.; Stubbs, C. D. *Biochemistry* **1995**, *34*, 6188−6195.
(58) Kelusky, E. C.; Smith, I. C. *Biochemistry* **1983**, *22*, 6011−6017.
(59) Shintou, K.; Nakano, M.; Kamo, T.; Kuroda, Y.; Handa, T. *Biophys. J.* **2007**, *93*, 3900−3906.
(60) Hornby, A. P.; Cullis, P. R. *Biochim. Biophys. Acta* **1981**, *647*, 285−292.
(61) Borkenhagen, L.; Kennedy, E. P.; Fielding, L. *J. Biol. Chem.* **1961**, *236*, PC28−PC30.
(62) Yeung, T.; Gilbert, G. E.; Shi, J.; Silvius, J.; Kapus, A.; Grinstein, S. *Science* **2008**, *319*, 210−213.
(63) Grenache, D. G.; Gronowski, A. M. *Clin. Biochem.* **2006**, *39*, 1−10.
(64) Seddon, A. M.; Lorch, M.; Ces, O.; Templer, R. H.; Macrae, F.; Booth, P. J. *J. Mol. Biol.* **2008**, *380*, 548−556.
(65) Ohmi, Y.; Tajima, O.; Ohkawa, Y.; Yamauchi, Y.; Sugiura, Y.; Furukawa, K.; Furukawa, K. *J. Neurochem.* **2011**, *116*, 926−935.
(66) Yu, R. K.; Tsai, Y. T.; Ariga, T. *Neurochem. Res.* **2012**, *37*, 1230−1244.
(67) Monson, C. F.; Cong, X.; Robison, A. D.; Pace, H. P.; Liu, C.; Poyton, M. F.; Cremer, P. S. *J. Am. Chem. Soc.* **2012**, *134*, 7773−7779.
(68) Nakagaki, M.; Katoh, I.; Handa, T. *Biochemistry* **1981**, *20*, 2208−2212.
(69) Castellana, E. T.; Cremer, P. S. *Biointerphases* **2007**, *2*, 57−63.
(70) Smith, K. A.; Gale, B. K.; Conboy, J. C. *Anal. Chem.* **2008**, *80*, 7980−7987.
(71) Rainsford, K. D. *Int. J. Clin. Pract.* **2013**, *67*, 9−20.
(72) Thun, M. J.; Jacobs, E. J.; Patrono, C. L. *Nat. Rev. Clin. Oncol.* **2012**, *9*, 259−267.
(73) Tahrani, A. A.; Piya, M. K.; Barnett, A. H. *Adv. Ther.* **2009**, *26*, 249−262.